CrystEngComm

COMMUNICATION

View Article Online
View Journal | View Issue

Cite this: *CrystEngComm*, 2025, **27**, 1248

Received 13th September 2024,
Accepted 21st January 2025

DOI: 10.1039/d4ce00937a

rsc.li/crystengcomm

Synthesis, structure, and stability of a novel 2*H*-azirine under pressure†

Alexa Cabrera, [a] Fatemah Safari, [b] Ravhi Kumar, [b] Haoran Zhu, [a] Muhtar Ahart, [b] Zhenxian Liu, [b] Tom G. Driver [a] and Russell J. Hemley [abc]

We have synthesized 2,3-diphenyl-2*H*-azirine, a strained unsaturated heterocyclic compound, and examined its high-pressure behavior to above 10 GPa using diamond anvil cell techniques. Single crystal X-ray diffraction at ambient conditions reveals that the crystal structure is hexagonal and consists of interesting helices surrounding voids in the structure. A continuous shift of the Raman and infrared vibrational spectra with increasing pressure is observed, indicating that the molecular structure is preserved to at least 8 GPa at room temperature. High-pressure synchrotron powder X-ray diffraction shows that the hexagonal structure persists, with a smooth compression of the *a* and *c* parameters to 10 GPa. The structural stability under pressure is attributed to the reduction in void size within the helical framework despite the inherent strain and reactivity of the molecule. The channels in the structure could encapsulate small molecules for gas or energy storage applications.

Introduction

2*H*-Azirines represent a unique class of organic compounds characterized by their remarkable strain and unsaturated three-membered ring structure housing a pivotal nitrogen atom. The ring strain of 2*H*-azirines imbues them with significant reactivity (ring strain calculated to be 44–47 kcal mol^{-1}).[1,2] The inherent strain in 2*H*-azirines renders them intriguing subjects of inquiry and endows them with exceptional reactivity, facilitating diverse transformations that potentially lead to complex organic architectures.[3] Scheme 1 shows the changes 2,3-diphenyl-2*H*-azirine could undergo. Photolysis of 2,3-diphenyl-2*H*-azirine 1 produces an irreversible ring opening through cleavage of the C–C bond to generate a nitrile ylide 2, and the direct observation of this reactive intermediate has been reported.[4–6] The resulting nitrile ylide can dimerize to afford tetraphenylpyrazine 3 or undergo cycloaddition with a range of dipolarophiles (X═Y) to afford pyrroline derivatives 4.[6–8] In contrast, thermolysis of 2*H*-azirines produces vinyl nitrene 5 through heterolysis of the C–N bond. This intermediate reacts with proximal C–H bonds to produce 2-substituted indoles 6.[9–11] This reactivity enables them to be positioned strategically as synthetic intermediates to facilitate the efficient production of a wide range of organic compounds with diverse applications across pharmaceuticals, agrochemicals, materials, and fine chemicals industries.[3,9,12–21]

Armed with new high-pressure tools, we wished to examine the stability and potential reactivity of 2,3-diphenyl-2*H*-azirine under pressure to determine at what/if any pressure triggers C–N or C–C bond cleavage and if this reactivity could be harnessed to generate novel nitrogen-rich high energy density materials (HEDMs).

Investigating the crystal and molecular structure of organic compounds over a range of thermodynamic conditions helps gain a deeper insight into their physical and chemical properties.[22,23] Subjecting molecular crystals to

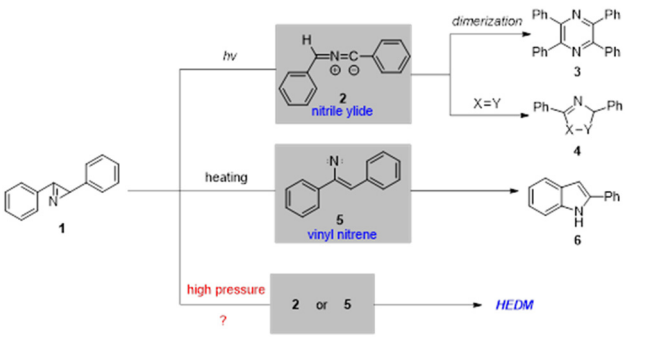

Scheme 1 Potential reactivity of 2*H*-azirines induced by light, temperature, and high pressure, the latter leading to possible high-energy density materials (HEDMs).

[a] *Department of Chemistry, University of Illinois Chicago, Chicago, IL 60607, USA. E-mail: rhemley@uic.edu*
[b] *Department of Physics, University of Illinois Chicago, Chicago, IL 60607, USA*
[c] *Department of Earth and Environmental Sciences, University of Illinois Chicago, Chicago, IL 60607, USA*

† Electronic supplementary information (ESI) available: CCDC 2380981. For ESI and crystallographic data in CIF or other electronic format see DOI: https://doi.org/10.1039/d4ce00937a

high pressures can dramatically affect crystal structures, reactivity, solubility, and melting behavior, even over relatively modest conditions up to several to tens of gigapascals.[24–26] The materials can be probed *in situ* with diamond-anvil cells using various techniques, most notably single-crystal and powder diffraction coupled with vibrational spectroscopies.[27–35] Furthermore, accurately determining pressure–volume (*P–V*) equations of state (EOS) can provide detailed information on compression mechanisms and thermodynamic properties.[36,37]

Despite this variety of organic compounds that have been examined under pressure, the behavior of 2*H*-azirines has yet to be examined. In this study, we present an investigation of compound 2,3-diphenyl-2*H*-azirine, which features a strained nitrogen-ring structure. We synthesized the 2*H*-azirine, determined its structure under ambient conditions, and assessed its high-pressure stability, structure, and vibrational properties using Raman spectroscopy, infrared spectroscopy, and X-ray diffraction up to 20 GPa. Rather than reacting or breaking down to known more stable molecules or transforming denser HEDMs, the structure persists to remarkably high compression. We attribute the stability of the material under pressure to the unusual spiral structure with voids that collapse. The findings have important implications for the high-pressure synthesis and properties of other HEDMs.

Results

Synthesis and structure

2,3-Diphenyl-2*H*-azirine was synthesized from phenyl benzyl ketone and sodium acetate (Fig. S1†).[38] Pressure was calibrated using the ruby-fluorescence method.[39] Single-crystal X-ray diffraction techniques at ambient conditions were used to reveal the atomic position of the compound. Crystal structure refinement yielded a hexagonal structure with lattice parameters a = 18.596(5) Å, c = 5.704(2) Å. 2,3-Diphenyl-2*H*-azirine is a nonlinear molecule with C_1 point group symmetry (Table 1). Due to the molecule's chirality, the crystal structure has a 6-fold translational symmetry that lacks a mirror plane, inversion center, and no rotational or reflection symmetry (*P*65 space group). The stacked crystallographic layers can be visualized by plotting the unit cell. The strained molecules show the interaction of the hydrogen bonds as the diphenyls are in close proximity. Surprisingly, the helices of 2,3 diphenyl-2*H*-azirine molecules are not connected by hydrogen bonds, and voids are formed in the corners of the unit cell (Fig. 1 and S2†).

Table 1 Crystallographic data for 2,3-diphenyl-2*H*-azirine ($C_{14}H_{11}N$) at 0.1 MPa/298 K

Pressure (GPa)	0.1 MPa
Space group	*P*65
Unit cell a (Å)	18.5963 (5)
b	18.5963 (5)
c	5.7039 (2)
γ (°)	120
Volume (Å^3)	1708.27 (11)
Z/Z'	6/1
D_x (g cm^{-3})	1.127

Raman spectroscopy

Raman spectra were measured as a function of pressure to examine compressional effects on the molecular stability, lattice and internal molecular vibrations, and possible pressure-induced phase transitions or chemical reactions in the solid state. The 2,3-diphenyl-2*H*-azirine molecule consists of 26 atoms, which gives rise to 72 vibrational modes that correspond to its C_1 point group, all of which are Raman-active. The *P*65 space group of the crystal structure gives rise to 432 zone-center vibrations, of which 387 are Raman-active ($77A + 77E_1 + 78E_2$).

Raman spectra were measured under pressure in several different runs. A 785 nm laser was used for these measurements because of the intense fluorescence of the sample with shorter wavelength laser lines (Fig. S3†).[40,41] A gradual increase in background fluorescence was observed with pressure using the 785 nm laser excitation (Fig. S4†). Nevertheless, well-defined Raman bands could be measured up to 8.3 GPa (Fig. 2a), including prominent modes initially at 149 and 615 cm^{-1} (azirine group twist and anti-symmetric stretch), ~997 and 1602 cm^{-1} (phenyl stretch and scissoring), 1747 cm^{-1} (N=C stretch). Peaks at lower frequencies were also observed but broadened on compression (Fig. S5†). Quantum calculations of the vibrational modes of the isolated molecules were used to guide the analysis. Specifically, we used the B3LYP/6-31G method in Gaussian 09 (ref. 42) to calculate the frequencies and displacements of the vibrational modes of the isolated molecule (Fig. S6†). From the predicted intensities, the 26 observed bands were tentatively assigned (Fig. 2b).

Infrared spectroscopy

High-pressure infrared spectroscopy was also used to provide information on molecular stability and possible pressure-induced changes in the material. In particular, both far-IR (50–700 cm^{-1}) and mid- to near-IR (700–5000 cm^{-1}) spectra were measured using synchrotron infrared techniques up to 20 GPa. Given the C_1 point group symmetry, all vibrational modes are both IR and Raman-active for the isolated molecule. To measure the 0.1 MPa spectrum, the sample was compressed as a thin pellet in which all absorption peaks could be identified without interference from diamond absorption (Fig. S7†). The high-pressure spectra reveal a substantial number of peaks indicating stability of the molecule up to at least 10 GPa (Fig. 3a). High-frequency peaks are observed that are readily identified as combination bands arising from the excitation of IR- and Raman-active modes at 4042 cm^{-1}, 4343 cm^{-1}, 4443 cm^{-1}, 4527 cm^{-1}, 4613 cm^{-1}, and 4657 cm^{-1} (Table S1†). For example, the IR-active ν_2 vibration is observed at 3083 cm^{-1}, and ν_4 appears in Raman at 1268 cm^{-1}. The 4343 cm^{-1} peak can thus be

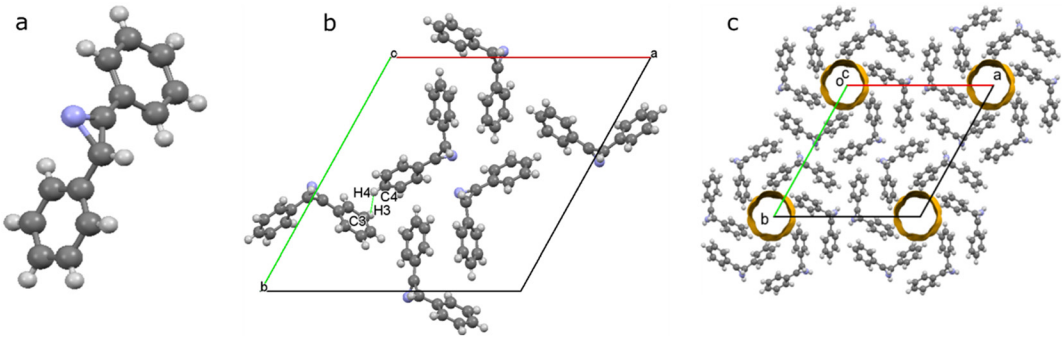

Fig. 1 (a) 2,3 Diphenyl-2*H*-azirine molecule. (b) Unit cell structure viewed along the *c*-direction, showing the distance between the C4B–H4B and C3A–H3A molecules (see text). (c) Expanded view of the structure along the *c*-axis showing the voids in the unit cell.

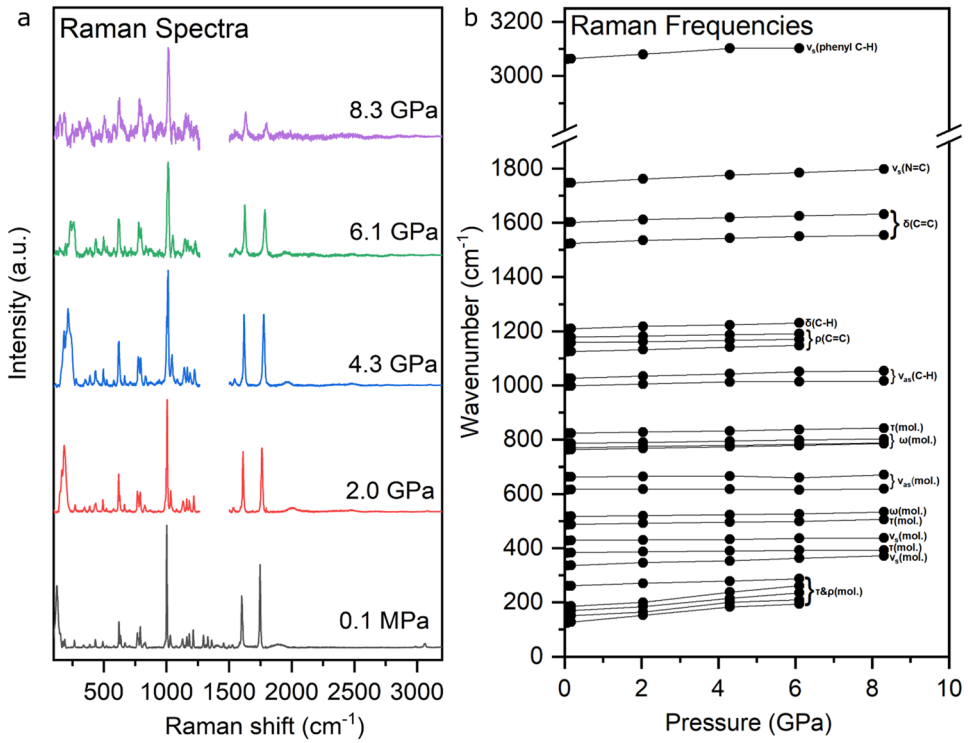

Fig. 2 (a) Raman spectra of 2,3-diphenyl-2*H*-azirine at selected pressures (785 nm laser excitation). The fluorescence background, which increased with increasing pressure, was subtracted in the higher pressure spectra, and signal in the vicinity of the strong T_{2g} Raman mode from the diamond anvils was removed in the high-pressure spectra. (b) Pressure dependence of the Raman frequencies, with the approximate vibrational modes assigned: molecular twist τ, rock ρ, wag ω, symmetric stretch ν_s, and asymmetric stretch ν_{as} modes; mol. indicates motion distributed over the entire molecule.

identified as a combination band of the ν_2 and ν_4 fundamentals (Table S1†). These positions of the combination bands confirm the identification and assignments of lower frequency Raman and IR modes.

High-pressure X-ray diffraction

High-pressure powder X-ray diffraction was also measured to further elucidate the diffraction and spectroscopic changes discussed above. The 2,3-diphenyl-2*H*-azirine was compressed up to 10.4 GPa with neon as a medium to investigate possible pressure-induced structural and chemical changes directly (Fig. S8 and S9†). The unit cell parameters obtained from the powder diffraction data agree with those obtained from the single crystal refinements. The evolution of X-ray diffraction patterns at various pressures is shown in Fig. 4a. The observed diffraction patterns were readily indexed to a hexagonal unit cell at each pressure. The diffraction peaks systematically shift with pressure with no evident splitting but some peak broadening is observed at the highest pressures. The *d*-spacings determined from the X-ray patterns are shown in Fig. 4b.

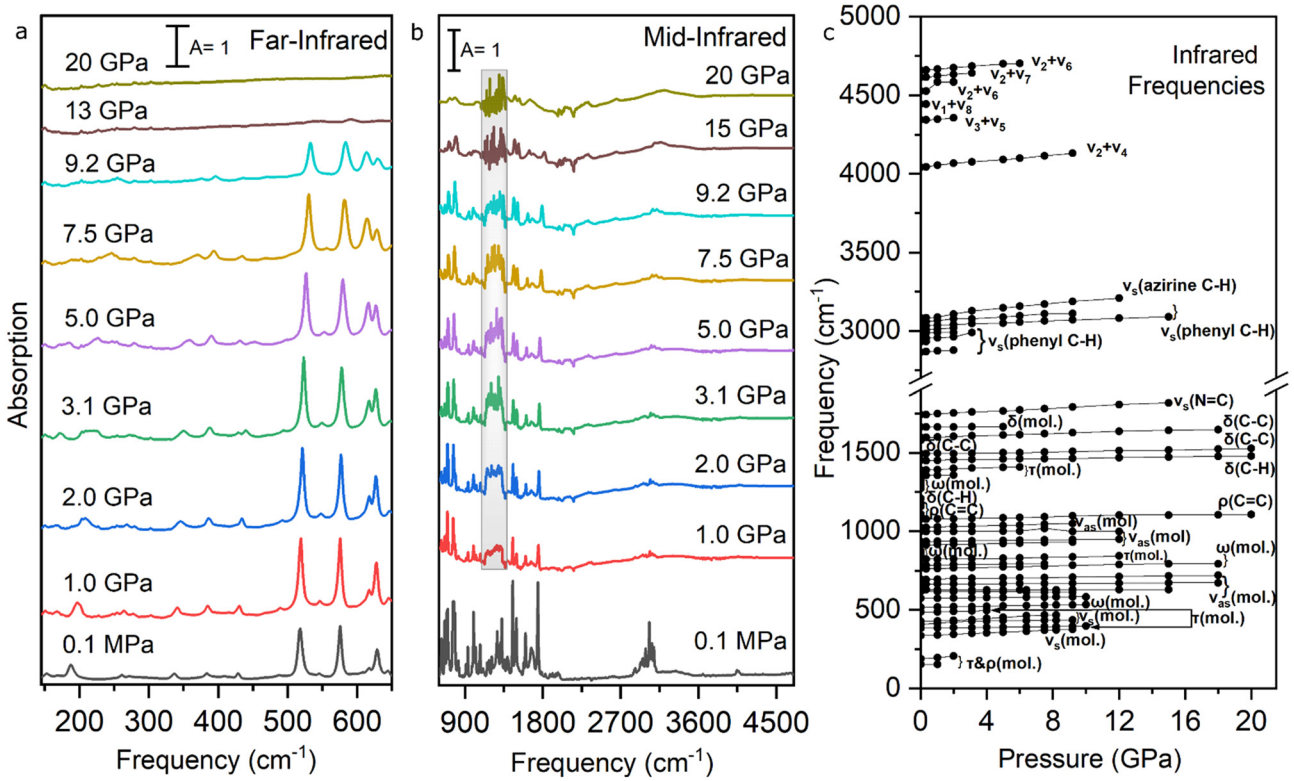

Fig. 3 (a) Selected far-infrared spectra of 2,3-diphenyl-2*H*-azirine measured with petroleum jelly pressure-transmitting medium. (b) Mid-IR spectra were measured with a KBr pressure-transmitting medium. The shaded area of the spectra corresponds to the region of background absorption from the diamond anvils. The ambient pressure (0.1 MPa) far- and mid-IR spectrum was measured on a pure sample. (c) Far- and mid-IR absorption frequencies plotted as a function of pressure with approximate assignments of the vibrational modes, including combination bands at 4000–4700 cm^{-1}.

The hexagonal unit-cell parameters a and c obtained from the analysis are shown in Fig. 5. There is a smooth compression of the hexagonal unit cell up to 10 GPa with no evidence of pressure-induced phase transitions or chemical reactions over the range of conditions explored.

Equation of state

The pressure–volume (P–V) data obtained from the X-ray diffraction were fitted to a third-order Vinet EOS (Fig. 6).[43] A Vinet equation of state fit of the entire pressure–volume data with a zero-pressure reference volume V_0 = 1708 Å^3 gives a bulk modulus K_0 and pressure derivative $K_0' = 8.4(1.5)$ of 6.2(1.6) GPa and 15.6(2.4), respectively. However, a single EOS fit does not accurately fit the data at lower pressure, introducing too much curvature at low compression. A superior fit of the data was obtained by dividing the data into two EOS regimes. A fit to the data from ambient pressure to 37 GPa gave K_0 = 10.6(1.2) GPa and K_0'. This analysis provides a much better fit to the lower pressure data as well as a more reasonable $K_0' = 18(5)$. The comparison suggests a slight change in the compression mechanism near 3.7 GPa. The fit to the higher-pressure data from 3.7 to 10.5 GPa gave K_0 = 3.9(2.4) GPa and $K_0' = 18(5)$. Despite the possible change in compression mechanism, the X-ray diffraction data reveal the persistence of hexagonal unit cell over the entire pressure range explored.

Discussion

We first discuss the stability of the molecule and molecular crystal structure on compression, beginning with the crucial evidence provided by the high-pressure Raman and IR spectra. Distinct features characteristic of intact azirine molecules persist to comparable pressures using both techniques; *i.e.*, at least 8 GPa in Raman and 9.2 GPa in IR. Measurements of the Raman spectra were complicated at higher pressure by background fluorescence, such that only faint vibrational peaks could be observed beginning at 12 GPa. In the IR, vibrational peaks were apparent at 20 GPa (although broadened at higher pressures). Spectra were also measured on decompression of the samples. Decompression from 12 GPa to ambient pressure revealed no visible azirine peaks due to the persistence of fluorescence (Fig. S10†). On the other hand, measurement of the IR spectrum on decompression from these pressures shows the persistence of azirine vibrations (Fig. S11†).

The *in situ* high-pressure X-ray diffraction measurements show that the compound persists in a hexagonal structure up to 10 GPa, the maximum pressure of these experiments.

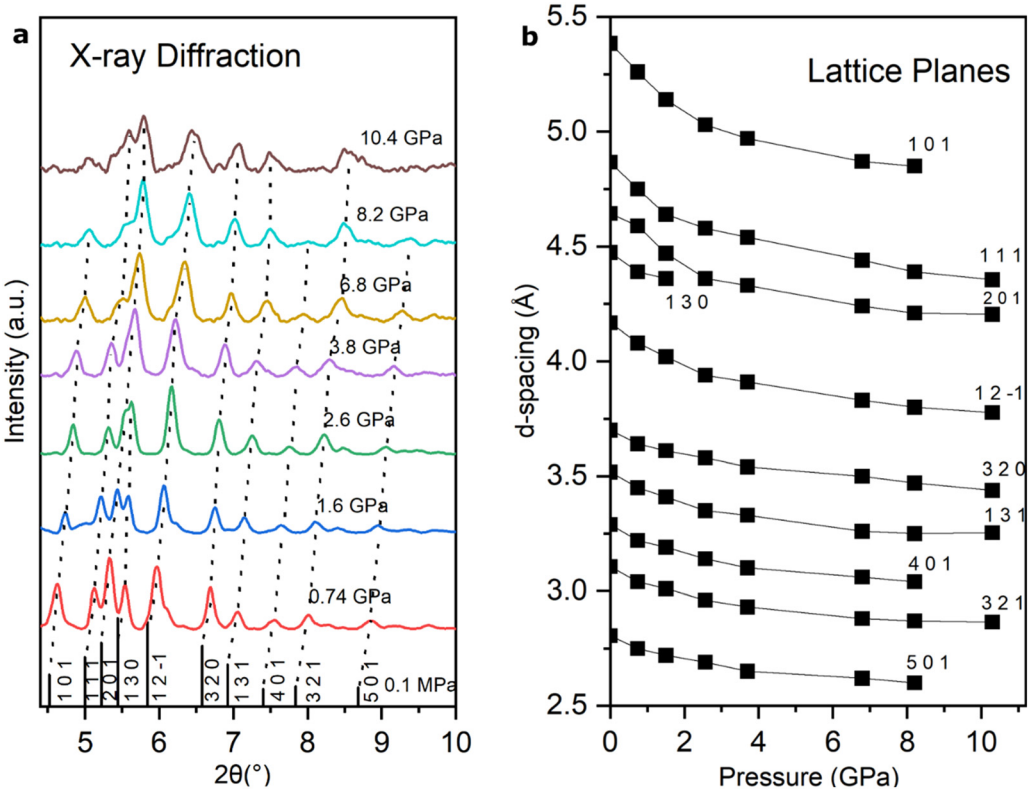

Fig. 4 (a) Selected synchrotron X-ray diffraction patterns as a function of pressure with major peaks labeled. Six principal peaks indexed with *hkl* values 111, 201, 12–1, 320, 131, and 321 are observed. (b) The *d*-spacing values obtained from the X-ray diffraction data are labeled with their Miller indices. The continuous decrease in *d*-spacings indicates no major change in the hexagonal structure on compression.

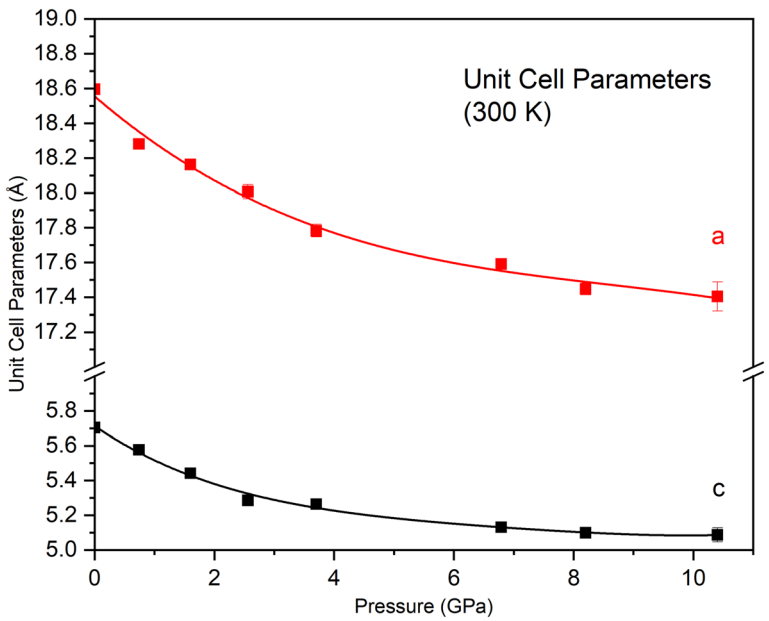

Fig. 5 Unit-cell parameters as a function of pressure for 2,3-diphenyl-2*H*-azirine measured by X-ray diffraction. The error bars are within the size of the data points.

At that pressure, the unit-cell volume is reduced by 22%, which is a notable degree of compression. The ambient pressure structure refined by single-crystal X-ray diffraction is characterized by the presence of voids within the structure, as noted above. We attribute the reduction in the volume under pressure without a phase transformation or chemical reaction to the shrinkage of the voids during compression.

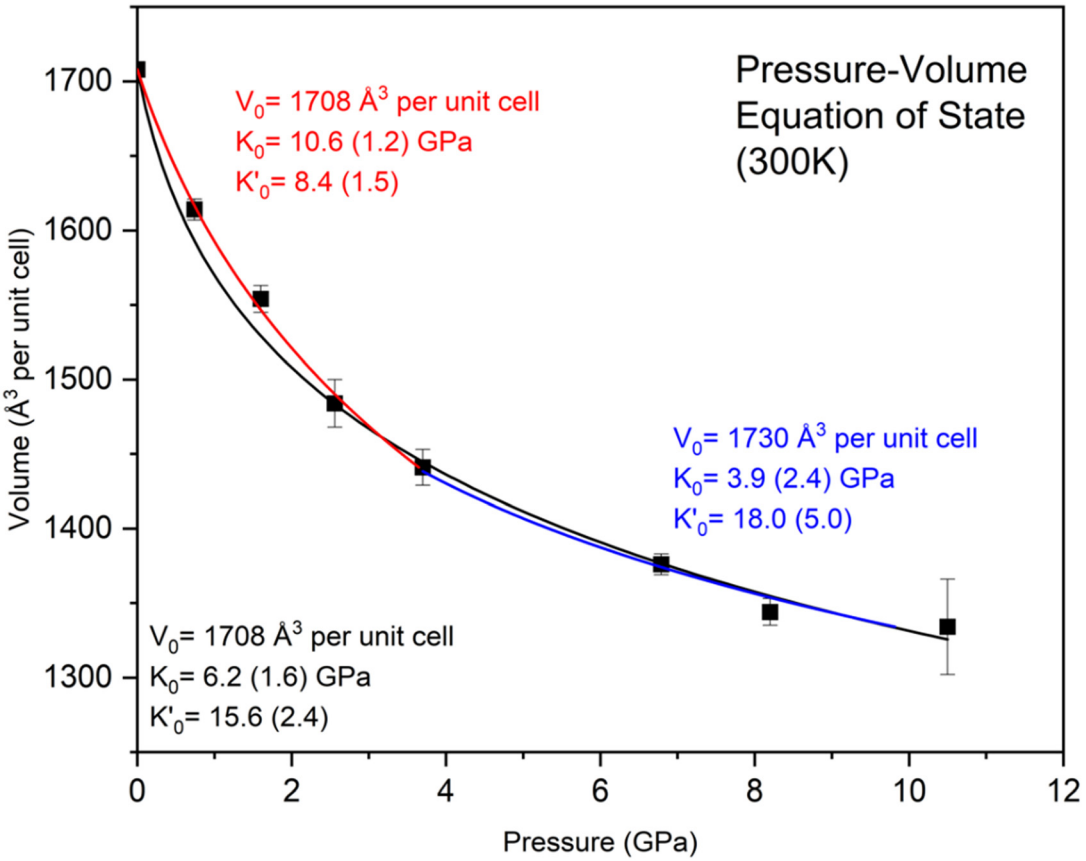

Fig. 6 *P–V* relations of 2,3-diphenyl-2*H*-azirine obtained from the X-ray diffraction. The black solid line shows a Vinet EOS fit of the entire data set, while the red line indicates the fit from ambient to 3.7 GPa, and the blue line shows the fit from 3.7 GPa to 10.5 GPa. The *P–V* data are listed in Table S2.†

Additional insight is gained by further examination of the crystal structure. The molecular arrangements in the unit cell show that adjacent molecules are perpendicular to each other, with C4B–H4B on top of C3A–H3A at a distance of 3.16 Å (Fig. 1b). Vibrational modes associated with the short C4B–H4B and C3A–H3A distances are expected to have a strong pressure dependence. We suggest that the vibrational bands with stronger pressure shifts are associated with displacements of the atoms mentioned above.

We compare our results with those of related molecular crystals under pressure. Comparing the parameters to other similar aromatic compounds can serve as an observation for compression behavior when analyzing the potential changes in the crystal structure.[44,45] The aromatic heterocyclic compound 2-phenylindole contains a pyrrole ring fused to a benzene ring.[46] The vibrational spectrum of indole was examined (Fig. S12b†) to compare with our results for the azirine (Fig. S12a†) and, in particular, to examine the evidence for azirine chemically transforming under pressure (Fig. S12c†). Notably, the azirine and indole have distinct spectra at ambient pressure. With increasing pressure, none of the peaks measured for the azirine matched those of the indole.

We also compare our results with those obtained for 4-hydroxycyanobenzene (4HCB), which has one phenyl group and thus potentially similar π–π and H-bonding interactions.[47] Notably the bulk moduli are close, with K_0 = 9.7(2) GPa for 4HCB compared to the best-fit K_0 = 10.6(1.2) GPa for the 2*H*-azirine. On the other hand, 4HCB undergoes two phase transitions over a similar pressure range, in contrast to the 2*H*-azirine, perhaps associated with the additional diphenyl group in the latter. Another related compound is paracetamol, which contains a phenyl group; it has two known polymorphs, monoclinic (form I) and orthorhombic (form II), with similar bulk moduli.[48] Like the azirine, no phase transition or chemical transformation was observed on compression of paracetamol (up to 4 GPa). These organic compounds give insight into the stability of related molecular structures on compression, with one remaining at its original structure and the other that did not. High-pressure study of such compounds and comparing their EOS allows a better understanding of the crystal packing in these and other compounds.[49–54]

Conclusions

2,3-Diphenyl-2*H*-azirine has been successfully synthesized and found to crystallize in a novel hexagonal structure at ambient conditions. High-pressure Raman and infrared

spectroscopy, together with high-pressure X-ray diffraction, reveal that the molecules and crystal structure remain stable up to the 10 GPa pressure range at room temperature. Despite the compound's inherent reactivity and molecular instability, this unexpected stability can be attributed to the unique crystal structure, which accommodates compression by reducing voids around the helical units in the hexagonal lattice. On the other hand, analysis of the *P–V* relation suggests a change in compression mechanism within the pressure range studied. Further study, including measurements at variable temperatures and high pressures, would provide additional information on the interatomic and intermolecular interactions as well as chemical reactions of the compound under varying thermodynamic conditions. In addition, the voids in the novel structure of the azirine could encapsulate small molecules for gas or energy storage applications. The results highlight how specific crystal structures can allow enhanced stability under pressure of molecules that may otherwise be considered to be highly chemically unstable.

Data availability

Crystallographic data supporting this article have been uploaded to CCDC as deposition #2380981.

Author contributions

T. D. and H. Z. synthesized the 2,3-diphenyl-2*H*-azirine and the 2-phenylindole. A. C. and F. S. performed the single-crystal XRD. A. C. and R. K. conducted the high-pressure XRD experiments. A. C. measured all the Raman spectra with the help of M. A. A. C. and Z. L. performed the IR measurements. R. J. H. supervised the project. All authors contributed to the preparation of the manuscript.

Conflicts of interest

There are no conflicts to declare.

Acknowledgements

This work was supported by Extreme EnErgy Density (EXEED), an Army HBCU/MI Center of Excellence at the University of Illinois Chicago, under grant #W911NF2110275 from the Army Research Office, and by the U.S. Department of Energy-National Nuclear Security Administration (DOE-NNSA) cooperative agreement DE-NA-0004153 (Chicago/DOE Alliance Center, CDAC). Synchrotron X-ray experiments were performed at HPCAT (Sector 16) Advanced Photon Source (APS), Argonne National Laboratory (ANL). HPCAT operations are supported by DOE-NNSA's Office of Experimental Sciences. The APS is a DOE Office of Science User Facility operated for the DOE Office of Science by ANL under contract DE-AC02-06CH11357. Synchrotron infrared experiments were performed at the Frontier Infrared Spectroscopy (FIS) at the National Synchrotron Light Source II (NSLS-II), Brookhaven National Laboratory (BNL). FIS is supported by DOE-NNSA (CDAC) and NSF cooperative agreement EAR-2223273 (Synchrotron Earth and Environmental Science, SEES). The NSLS-II is a DOE Office of Science User Facility operated by the DOE Office of Science by BNL under contract DE-SC0012704.

Notes and references

1 S. Calvo-Losada, *J. Comput. Chem.*, 1998, **19**, 912–922.
2 A. Rey Planells and A. Espinosa Ferao, *Inorg. Chem.*, 2022, **61**, 6459–6468.
3 A. F. Khlebnikov, M. S. Novikov and N. V. Rostovskii, *Tetrahedron*, 2019, **75**, 2555–2624.
4 A. Padwa, M. Dharan, J. Smolanoff and S. Wetmore, *Pure Appl. Chem.*, 1973, **33**, 269–284.
5 P. Claus, Th. Doppler, N. Gakis, M. Georgarakis, H. Giezendanner, P. Gilgen, H. Heimgartner, B. Jackson, M. Märky, N. S. Narasimhan, H. J. Rosenkranz, A. Wunderli, H. Hanse and H. Schmid, *Pure Appl. Chem.*, 1973, **33**, 339–362.
6 A. Padwa, S. Clough, M. Dharan, J. Smolanoff and S. I. Wetmore, *J. Am. Chem. Soc.*, 1972, **94**, 1395–1397.
7 A. Padwa, M. Dharan, J. Smolanoff and S. Wetmore, *J. Am. Chem. Soc.*, 1973, **95**, 1954–1961.
8 A. Padwa, J. Smolanoff and A. Tremper, *J. Am. Chem. Soc.*, 1975, **97**, 4682–4691.
9 L. A. Wendling and R. G. Bergman, *J. Org. Chem.*, 1976, **41**, 831–836.
10 D. F. Taber and W. Tian, *J. Am. Chem. Soc.*, 2006, **128**, 1058–1059.
11 X. Li, Y. Du, Z. Liang, Y. Pan and K. Zhao, *Org. Lett.*, 2009, **11**, 2643–2646.
12 P. A. Sakharov, M. S. Novikov and N. V. Rostovskii, *Chem. Heterocycl. Comp.*, 2021, **57**, 512–521.
13 E. Babaoglu and G. Hilt, *Chem. – Eur. J.*, 2020, **26**, 8879–8884.
14 C. K. Skipper, D. S. Dalisa and T. F. Molinski, *Bioorg. Med. Chem. Lett.*, 2010, **20**, 2029–2032.
15 C. K. Skepper, D. S. Dalisay and T. F. Molinski, *Org. Lett.*, 2008, **10**, 5269–5271.
16 J. L. Keffer, A. Plaza and C. A. Bewley, *Org. Lett.*, 2009, **11**, 1087–1090.
17 A. Padwa, *Adv. Heterocycl. Chem.*, 2010, **99**, 1–31.
18 E. Orton, S. T. Collins and G. C. Pimentel, *J. Phys. Chem.*, 1986, **90**, 6139–6143.
19 L. A. Wendling and R. G. Bergman, *J. Am. Chem. Soc.*, 1974, **96**, 308–309.
20 M. J. Alves and F. Texeira e Costa, in *Heterocyclic Targets in Advanced Organic Synthesis*, ed. M. Carreiras and J. Marco-Contelles, Research Signpost, Kerala, India, 2011, vol. 37(661), pp. 145–172.
21 G. S. Singh, M. D'hooghe and N. De Kimpe, *Chem. Rev.*, 2007, **107**, 2080–2135.
22 G. R. Desiraju, *J. Am. Chem. Soc.*, 2013, **135**, 9952–9967.
23 S. J. Maginn and G. R. Desiraju, *J. Appl. Crystallogr.*, 1991, **24**, 265.

24 E. Boldyreva, *Z. Kristallogr. - Cryst. Mater.*, 2014, **229**, 236–245.
25 A. Healy, Z. Worku, D. Kumar and A. Madi, *Adv. Drug Delivery Rev.*, 2017, **117**, 25–46.
26 J. A. Ciezak, T. A. Jenkins, Z. Liu and R. J. Hemley, *J. Phys. Chem. A*, 2007, **111**, 59–63.
27 E. V. Boldyreva, *J. Mol. Struct.*, 2003, **647**, 159–179.
28 E. V. Boldyreva, *Cryst. Eng.*, 2003, **6**, 235–254.
29 E. V. Boldyreva, H. Ahsbahs and H. P. Weber, *Z. Kristallogr. - Cryst. Mater.*, 2003, **218**, 231–236.
30 E. V. Boldyreva, T. P. Shakhtshneider, H. Ahsbahs, H. Sowa and H. Uchtmann, *J. Therm. Anal. Calorim.*, 2002, **68**, 437–452.
31 E. V. Boldyreva, V. A. Drebushchak, I. E. Paukov, Y. A. Kovalevskaya and T. N. Drebushchak, *J. Therm. Anal. Calorim.*, 2004, **77**, 607–623.
32 A. Katrusiak, *Acta Crystallogr., Sect. B*, 1995, **51**, 873–879.
33 A. Katrusiak, *Acta Crystallogr., Sect. B*, 1990, **46**, 246–256.
34 A. Katrusiak, *High Pressure Res.*, 1991, **6**, 265–275.
35 A. Botteon, M. Vermeulen, L. Cristina, S. Bruni, P. Matousek, C. Miliani, M. Realini, L. Angelova and C. Conti, *Anal. Chem.*, 2024, **96**, 4535–4543.
36 E. Stavrou, M. R. Manaa, J. M. Zaug, I. Kuo, P. F. Pagoria, B. Kalkan, J. C. Crowhurst and M. R. Armstrong, *J. Chem. Phys.*, 2015, **143**, 144506.
37 F. J. Zerilli and M. M. Kuklja, *J. Phys. Chem. A*, 2007, **111**, 1721–1725.
38 Y. Wang, X. Lei and Y. Tang, *Chem. Commun.*, 2015, **51**, 4507–4510.
39 H. Mao, J. Xu and P. M. Bell, *J. Geophys. Res., B*, 1986, **91**, 4673–4676.
40 E. P. Huang, E. Huang, S. Yu, Y. Chen and J. Lee, *Mater. Lett.*, 2010, **64**, 580–582.
41 G. Qi, K. Wang, K. Yang and B. Zou, *J. Phys. Chem. C*, 2016, **120**, 21293–21298.
42 M. J. Frisch, G. W. Trucks, H. B. Schlegel, G. E. Scuseria, M. A. Robb, J. R. Cheeseman, G. Scalmani, V. Barone, B. Mennucci, G. A. Petersson, H. Nakatsuji, M. Caricato, X. Li, H. P. Hratchian, A. F. Izmaylov, J. Bloino, G. Zheng, J. L. Sonnenberg, M. Hada, M. Ehara, K. Toyota, R. Fukuda, J. Hasegawa, M. Ishida, T. Nakajima, Y. Honda, O. Kitao, H. Nakai, T. Vreven, J. A. Montgomery, Jr., J. E. Peralta, F. Ogliaro, M. Bearpark, J. J. Heyd, E. Brothers, K. N. Kudin, V. N. Staroverov, R. Kobayashi, J. Normand, K. Raghavachari, A. Rendell, J. C. Burant, S. S. Iyengar, J. Tomasi, M. Cossi, N. Rega, J. M. Millam, M. Klene, J. E. Knox, J. B. Cross, V. Bakken, C. Adamo, J. Jaramillo, R. Gomperts, R. E. Stratmann, O. Yazyev, A. J. Austin, R. Cammi, C. Pomelli, J. W. Ochterski, R. L. Martin, K. Morokuma, V. G. Zakrzewski, G. A. Voth, P. Salvador, J. J. Dannenberg, S. Dapprich, A. D. Daniels, Ö. Farkas, J. B. Foresman, J. V. Ortiz, J. Cioslowski and D. J. Fox, *Gaussian 09*, Gaussian, Inc., Wallingford, CT, 2009.
43 P. Vinet, J. Ferrante, J. H. Rose and J. R. Smith, *J. Geophys. Res., B*, 1987, **92**, 9319–9325.
44 O. Franco, G. Reck, I. Orgzall and B. Schulz, *J. Phys. Chem. Solids*, 2002, **63**, 1805–1813.
45 C. Weidenthaler, T. J. Frankcombe and M. Felderhoff, *Inorg. Chem.*, 2006, **45**, 3849–3851.
46 S. S. El-Nakkady, M. M. Hanna, H. M. Roaiah and I. A. Ghannam, *Eur. J. Med. Chem.*, 2012, **47**, 387–398.
47 I. E. Collings and M. Hanfland, *Molecules*, 2019, **24**, 1759.
48 E. V. Boldyreva, H. Sowa, H. Ahsbahs, S. V. Goryainov, V. V. Chernyshev, V. P. Dmitriev, Y. V. Seryotkin, E. N. Kolesnik, T. P. Shakhtshneide, S. N. Ivashevskaya and T. N. Drebushchak, *J. Phys.: Conf. Ser.*, 2008, **121**, 022023.
49 Agilent, *CrysAlis^{Pro} Software System (1.171.36.28)*, Agilent Technologies UK Ltd, Oxford, UK, 2013.
50 G. M. Sheldrick, *Acta Crystallogr., Sect. C: Struct. Chem.*, 2015, **71**, 3–8.
51 C. F. Macrae, P. R. Edgington, P. McCabe, E. Pidcock, G. P. Shields, R. Taylor, M. Towler and J. Van de Streek, *J. Appl. Crystallogr.*, 2006, **39**, 453–457.
52 J. Gonzalez-Platas, M. Alvaro, F. Nestola and R. Angel, *J. Appl. Crystallogr.*, 2016, **49**, 1377–1382.
53 G. Novak and A. Colville, *Am. Mineral.*, 1989, **74**, 488–490.
54 R. J. Hemley and P. Dera, *Rev. Mineral. Geochem.*, 2001, **41**, 335–419.